Nanoscale

PAPER

View Article Online
View Journal | View Issue

Cite this: *Nanoscale*, 2024, **16**, 21011

Interlaboratory comparison of endotoxin contamination assessment of nanomaterials†

Gary Hannon, *[a,b] Bethany J. Heaton, [c,d] Alexander Plant-Hately, [c,d] Christopher David, [c,d] Neill J. Liptrott, [c,d] Ainhoa Egizabal, [e] Ana Ayerdi-Izquierdo, [e] Noelia Alvarez, [e] Oihane Ibarrola, [f] Andres Arbona Celaya, [f] Angel Del Pozo Perez, [f] Nerea Lazcanoiturburu, [f] Iris Luzuriaga, [f] Fikirte Debebe Zegeye, [g] Shanbeh Zienolddiny-Narui, [g] An Jacobs, [h] Alexandra Van Driessche, [h] Inge Nelissen, [h] Ibane Abasolo, [i,j,k] Fernanda Andrade, [i,j] Nora Ventosa, [j,l] Elisabet González-Mira, [j,l] Aida Carreño [j,l] and Adriele Prina-Mello *[a,b,m]

Endotoxin contamination is a significant hurdle to the translation of nanomaterials for biomedical applications. Multiple reports now describe that more than one-third of nanomaterials fail early pre-clinical assessment due to levels of endotoxin above regulatory requirements. Additionally, most immunological studies or *in vivo* studies testing nanomaterials in the literature lack inclusion of this assessment, which may lead to false-positive or false-negative results if high levels of the contaminant are present. The currently approved methods for endotoxin contamination assessment rely on enzymatic activity and wavelength absorbance as their endpoint, and many nanomaterials can interfere with such assays. For this reason, we devised an interlaboratory comparison of endotoxin contamination assessment for a range of nanomaterials to challenge the current international organization for standardization and pharmacopeia standards. Herein, we show that detected endotoxin levels could vary considerably between groups, and, in some instances, nanomaterials could both pass and fail regulatory endotoxin limits for medical devices depending on the group undertaking the assessment, all while passing all quality criteria standards. This work emphasises the requirement for multiple assays to fully assess the endotoxin levels in a nanomaterial and highlights the need for additional assays to be developed in this space.

Received 8th July 2024,
Accepted 7th October 2024

DOI: 10.1039/d4nr02821j

rsc.li/nanoscale

Introduction

Nanomaterials (NM) possess unique physicochemical properties that make them attractive tools for many biomedical applications.[1] These novel characteristics also come with caveats, however, as their translation comes with many added challenges compared to conventional drugs.[2] One such safety hurdle for NM is endotoxin contamination. The large surface-to-volume ratios and multi-component design associated with NM can accommodate high levels of endotoxin. Additionally,

[a]*Nanomedicine and Molecular Imaging Group, Department of Clinical Medicine, Trinity Translational Medicine Institute, Trinity College Dublin, Dublin, Ireland. E-mail: prinamea@tcd.ie*
[b]*Laboratory of Biological Characterization of Advanced Materials (LBCAM), Trinity Translational Medicine Institute, Trinity College Dublin, Dublin, Ireland*
[c]*Immunocompatibility Group, Department of Pharmacology and Therapeutics, Institute of Systems, Molecular, and Integrative Biology, University of Liverpool, Liverpool, UK*
[d]*Centre of Excellence for Long-Acting Therapeutics, Department of Pharmacology and Therapeutics, Institute of Systems, Molecular, and Integrative Biology, University of Liverpool, Liverpool, UK*
[e]*TECNALIA, Basque Research and Technology Alliance (BRTA), Mikeletegi Pasealekua 2, 20009 Donostia-San Sebastián, Spain*
[f]*Biokeralty Research Institute AIE, Parque Tecnológico de Álava, Vitoria- Gasteiz, Álava, Spain*
[g]*National Institute of Occupational Health, Oslo, Norway*
[h]*Health department, Flemish Institute for Technological Research (VITO), Mol, Belgium*
[i]*Drug Delivery & Targeting, Vall d'Hebron Institute de Recerca (VHIR), Universitat Autònoma de Barcelona (UAB), 08035 Barcelona, Spain*
[j]*Networking Research Centre for Bioengineering, Biomaterials, and nanomedicine (CIBER-BBN), Instituto de Salud Carlos III, 28029 Madrid, Spain*
[k]*Functional Validation & Preclinical Research (FVPR)/U20 ICTS Nanobiosis, Vall d'Hebron Institut de Recerca (VHIR), Universitat Autònoma de Barcelona (UAB), 08035 Barcelona, Spain*
[l]*Institut de Ciència de Materials de Barcelona, ICMAB-CSIC, Campus UAB, 08193 Bellaterra, Spain*
[m]*Advanced Materials and Bioengineering Research (AMBER) Centre, CRANN Institute, Trinity College Dublin, Dublin, Ireland*

† Electronic supplementary information (ESI) available. See DOI: https://doi.org/10.1039/d4nr02821j

endotoxin's structure facilitates binding to both hydrophobic and cationic structures and its high thermal stability makes it incredibly difficult to remove once bound.[3] Intravenous injections of 2–4 ng kg^{-1} of endotoxin have consistently induced systemic inflammation in humans,[4,5] while lower doses (0.3 ng kg^{-1}) have been associated with low-grade inflammation.[6] Therefore, endotoxin represents a significant early safety consideration for NM.

In 2013, the National Cancer Institute's Nanotechnology Characterization Laboratory (NCI-NCL) reported that more than one-third of the nanomedicines they tested during a one-year period failed endotoxin contamination assessment.[7] More recently, another group published similar findings.[3] In addition to its high prevalence on NM, there is also evidence to suggest that the vast majority of publications detailing immunological assessments and *in vivo* studies with NM lack inclusion of endotoxin contamination assessment, potentially resulting in misleading findings.[8] Hence, endotoxin is a commonly overlooked, early hurdle to the translation of NM for biomedical applications.[9–11]

Testing for endotoxin contamination on NM is not a trivial endeavour, with the unique physicochemical properties of NM commonly leading to issues with assay interference.[12,13] The surface chemistry of NM can interfere with the constituents of the assay, while their optical properties commonly overlap with absorbance endpoints in these tests.[3,14] Accordingly, current international and Pharmacopeia standards for endotoxin testing require the inclusion of an inhibition-enhancement control (IEC) on top of common acceptance criteria to account for this potential interference.[15,16] The IEC is a spike-recovery control consisting of a known concentration of endotoxin spiked into a NM test sample that is subsequently detected to determine its propensity to introduce an inhibition or enhancement into the assay. An inhibition is considered a spike-recovery <50% of the concentration introduced, whereas an enhancement is defined as >200%.[13] However, despite this additional interference control, different results between assays have been reported.[12,17]

Here we present the results from an interlaboratory comparison (ILC) by the SAFE-N-MEDTECH (safety testing in the life cycle of nanotechnology-enabled medical technologies for health) consortium for the endotoxin contamination assessment of three NM and a medical implant coated with a nanosurface. These NM were analysed for their physicochemical characteristics (PCC) and tested for endotoxin contamination by eight different groups -including a Good Laboratory Practice (GLP) certified laboratory- using either the chromogenic, turbidimetric or gel clot *Limulus* amoebocyte lysate (LAL) assays or the recombinant factor C assay. Results showed that while no changes in PCC occurred during shipment, detected endotoxin levels could differ considerably between groups. Importantly, some of these differences could result in a NM both passing and failing regulatory requirements for a medical device, even when the same LAL assay is used. This study highlights potential issues with the currently accepted standards for endotoxin contamination of NM.

Materials and methods

Materials

The four chosen NM used for this study were (I) iron oxide nanoparticles (IONP) purchased from Chemicell GmbH (Germany) and consisted of a maghemite core with dextran coating and dispersed in water; (II) gold nanoparticles (GNP) purchased from NanoComposix, USA and were coated in polyethylene glycol and dispersed in water; (III) polystyrene nanoparticles (PsNP) purchased from Sigma Aldrich, Ireland and were also dispersed in water; and (IV) titanium-coated femoral hip stem medical device implant with a hydroxyapatite nanosurface purchased from Stryker Orthopaedics, Ireland. These four materials were utilised for the ILC as they all possessed a NM-component in their design and they varied in their structural, optical and chemical properties which enabled a robust comparison of the different endotoxin detection methods. The suppliers for all endotoxin detection kits are outlined in ESI Table 1.† Additionally, LAL reagent water (<0.001 EU ml^{-1} and <1.56 pg ml^{-1} (1,3)-β-D-glucan) used for aliquoting the solutions was supplied by Associates of Cape Cod Incorporated, United Kingdom.

Methods

Sample preparation for shipment. The four chosen samples were prepared for shipment to the consortium by the study coordinator and were assessed for their size distribution, surface charge and microbial contamination prior to shipment to serve as a baseline for the consortium (each method is described in detail in the subsequent paragraphs).

The IONP were supplied at 25 mg ml^{-1} stock concentration and then diluted to 10 mg ml^{-1} in LAL reagent water to ensure sufficient sample volume for the consortium. The GNP were supplied as a stock solution of 0.053 mg ml^{-1} concentration and were not diluted any further as sufficient volume was available as stock. The PsNP were also diluted from 100 mg ml^{-1} to 50 mg ml^{-1} concentration using LAL reagent water to provide enough sample volume for the consortium. The implant was completely submerged in 100 ml LAL reagent water for 24 h. After this time, the 'implant fluid' (or IF) was extracted and used to indirectly test the levels of endotoxin on the structure. Each sample was aliquoted into 5 ml pyrogen-free Eppendorf ™ tubes (Fisher Scientific, Ireland) for subsequent testing and sealed with Parafilm® M (Sigma Aldrich, Ireland) to avoid environmental exposure around the screw cap. The samples were then ready to be shipped to the consortium.

For shipment, samples were placed in sealed polystyrene boxes containing cold packs at 2–6 °C and arrived at their respective destinations within 24 hours. Upon arrival, samples were immediately stored at 2–6 °C until testing by the various partners.

Interlaboratory study design. This interlaboratory study was conducted according to International Organization for Standardization (ISO) 13528:2015: 'statistical methods for use in proficiency testing by interlaboratory comparison'. The three nanoparticle samples (IONP, GNP and PsNP) were tested,

prior to shipping and after aliquoting, by the study coordinator for their size distribution using nanoparticle tracking analysis (NTA) and dynamic light scattering (DLS). As described above, the samples were then shipped to each ILC partner for subsequent size and contamination testing. Each laboratory (excluding the GLP laboratory) then tested the NM for their size distribution with either NTA or DLS -under the same conditions as the study coordinator, and in accordance with European Union Nanomedicine Characterisation Laboratory (EUNCL) protocols[18,19]- to confirm the integrity of the samples had not been altered during shipping. Following size distribution assessment, the results were compared to ensure minimal differences in mean size (<10% coefficient of variance (CV)) and the samples were tested for endotoxin contamination by each group in at least one assay using the chromogenic, turbidimetric or gel clot LAL assays or the recombinant factor C assay according to ISO and Pharmacopeia standards.[15,16] The results for the endotoxin testing were compared statistically to determine differences between results (Fig. 1).

Nanoparticle tracking analysis. Initially, the diluent (American Chemical Society grade water; Lennox Laboratory Supplies Ltd, Dublin, Ireland) was filtered using rapid-flow sterile filters with a pore size of 0.2 μm (Thermo Scientific Nalgene, Dublin, Ireland). This was then measured with 3 × 60 s recordings using the NS500 Nanosight (Malvern-Panalytical, United Kingdom) to ensure no background interference. When confirmed, 100 nm polystyrene nanoparticle size calibration standard (Malvern Panalytical, United Kingdom) was measured. ±10% of this stated mean size range was deemed acceptable after 3, 60 s recordings. Next, the NM were diluted until 20–100 particles per frame were observed and then measured with a minimum of 3 × 60 s recordings with constant camera level of 12 and detection threshold of 5 for the IONP's (measurements), level of 7 and threshold of 5 for the GNP's and level of 11 and threshold of 5 for the PsNP's.

Dynamic light scattering- size distribution. As for NTA measurements, a particle-free diluent was used to dilute the NM to a suitable concentration. Once again, 100 nm polystyrene nanoparticle standard was measured as a quality control with the Nano- ZS (Malvern-Panalytical, United Kingdom) using disposable polystyrene cuvettes and an analysis involving 10 measurements of 12 runs, 10-second run duration, scattering angle of 173°, automatic attenuation selection and general-purpose analysis mode. As before, ±10% of this stated mean size range was deemed acceptable. A refractive index of 2.42 and absorbance of 0.029 was selected for the IONP's, index of 3 and absorbance of 0.03 for the GNP's and index of 1.59 and absorbance of 0.01 for the PsNP's.

Dynamic light scattering – zeta potential. Zeta potential was measured using the Zetasizer Nano Z (Malvern-Panalytical, United Kingdom). Each NM was diluted 1 : 100 in Milli-Q® Type 1 ultrapure water (Wasserlab, QA03DP30GR model) and measured for surface zeta potential using a minimum of

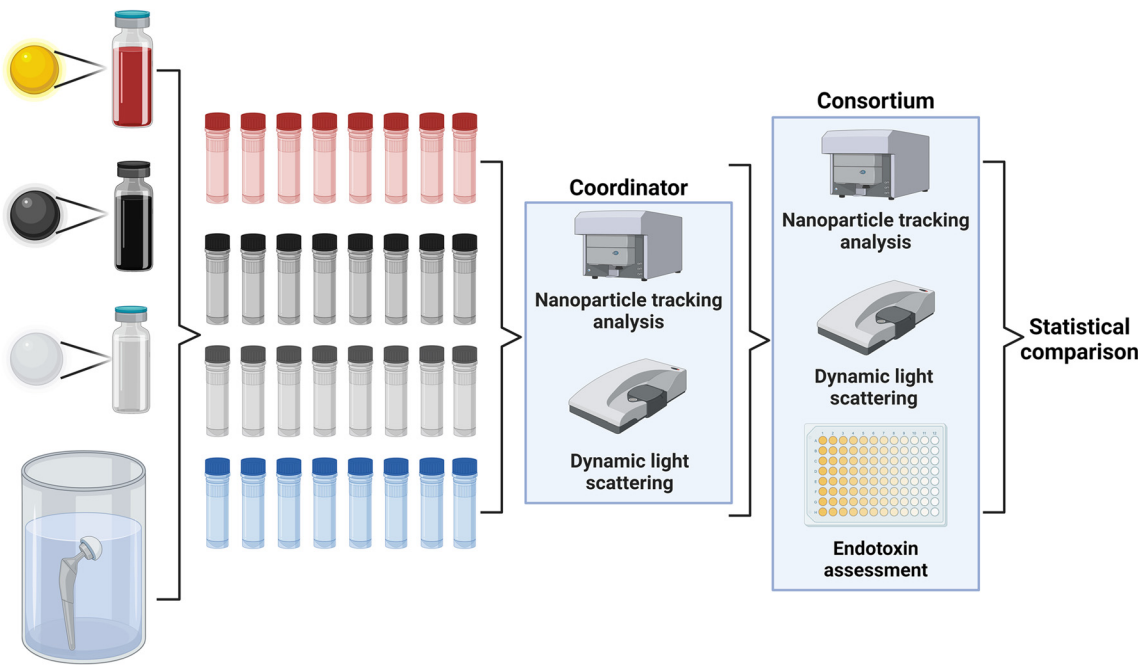

Fig. 1 Schematic workflow for the interlaboratory study. Stocks of IONP, GNP, PsNP and implant fluid are aliquoted into tubes and the samples tested by the study coordinator for size distribution by nanoparticle tracking analysis (NTA) and dynamic light scattering (DLS). The 4 samples were then shipped to 7 additional groups within the consortium who repeated the size distribution analysis of the samples with either NTA or DLS and also undertook endotoxin contamination assessment with a least one assay along with the coordinator. The size distribution and endotoxin contamination levels were statistically compared across all groups. [Note: size distribution analysis was not undertaken by the GLP laboratory prior to endotoxin testing].

3 measurements of 3 runs. Cuvettes used were Malvern's disposable folded capillary tubes (DTS1070). Equilibrium times lasted 120 seconds and 20-second delays were employed between measurements. Attenuation and voltage selection were automatic and analysis was also undertaken in automatic mode. Each measurement met Malvern's quality criteria for average count rate, phase plot and frequency plot.

Microbial contamination assessment. Microbial content of each sample was determined using Luria Broth Agar Plates (Lennox, Sigma Aldrich, Spain) and the assessment was conducted according to the EUNCL protocol.[20] Sterile water was used as a negative control and *E. coli* bacteria (Invitrogen, Spain) at a dilution of 10^{-7} from the stock (to enable counting and allow for ≥10 colony forming units (CFU) ml^{-1}) was used as a positive control. Spike-recovery controls were included in the analysis to assess possible interference of the samples with the assay by spiking each with bacteria at the same dilution as the positive control. 50 μl of each sample was applied to the surface of the agar plates in triplicate under sterile conditions (laminar flow cabinet) and the plates were incubated at 37 °C for 72 h. After counting the CFU present in the plates, the concentration was calculated based on the stock concentration of the sample tested. Additionally, the recovery percentage of spiked samples were also determined based on the difference of CFU between spiked samples and the positive control.

Mycoplasma contamination assessment. MycoAlert™ Mycoplasma Detection Kit (Lonza, Belgium) was used to determine the mycoplasma levels in each sample. Here, IONP and PsNP were diluted to 1 mg ml^{-1} and the IF and GNP were used at their stock concentration. 1 ml of each sample was added to 9 ml of cell culture media and applied to 80% confluent A549 cells (ATCC; LGC standards, Cedex, France) in a T25 flask. PBS at 1 ml (stock) in 9 ml of cell culture media was used as a negative control. The cells were incubated in duplicate with these treatments for 24 h, where they were then washed with PBS and fresh media replenished without antibiotic supplement. Viability was assessed at this point using a nucleocounter (Chemometec, United Kingdom) by dividing the total cell count by the dead cell count to ensure the concentrations of samples used were not cytotoxic. The cells were then passaged 3 more times into new T25 flasks once confluent using the antibiotic-free media. After the third passage, and once the media had been in contact with the cells for one week, 2 ml of the media was collected to be tested for mycoplasma contamination. This media was centrifuged for 5 minutes at 200*g*. The supernatants were then transferred to sterile sample tubes and 100 μl of each sample was added to a 96 well plate. 100 μl of lyophilized MycoAlert™ assay control was also added in duplicate to act as a positive control. 100 μl MycoAlert™ substrate reagent was then added to all sample wells and plate luminescence was read twice (before and after substrate addition) using a Luminometer (BMG Labtech, Netherlands) and the ratio between the first and second reading was used to determine mycoplasma concentration in each sample. As per the kit guidelines: a ratio <0.9 is considered a negative result, 0.9–1.2 indicates the cells should be tested again in 24 h and >1.2 is considered positive for mycoplasma contamination.

Beta-glucan assay. The Glucatell® kit from Associates of Cape Cod Incorporated, United Kingdom was used to determine (1, 3)-β-D-glucan (beta-glucan) levels in the samples. Here, the Glucatell® standard was reconstituted in LAL reagent water and a standard curve was created from 0–40 pg ml^{-1} of beta-glucan with 50 μl of each standard added to a 96 well plate in duplicate. Additionally, the samples at dilutions of 2× for the GNP, 100× for the IONP, 1000× for the PsNP and the undiluted stock for the IF were added to the 96 well plate at 50 μl in duplicate. A spike recovery control was also included for this assay, where 10 pg ml^{-1} of beta-glucan was spiked into each sample along with 10 pg ml^{-1} on its own as a quality control to determine whether each sample interferes with the assay. Once all samples and controls were added to the plate, the Glucatell® reagent was dispersed in Pyrosol® reconstitution buffer and 50 μl was added to each well, including a blank control. The plate was then heated to 37 °C for 30 minutes and a stop solution was then added to each well consisting of 50 μl sodium nitrite, 50 μl ammonium sulfamate and 50 μl of *N*-(1-napthyl) ethylenediamine dihydrochloride respectively. The plate was then read at 550 nm using an Epoch microplate reader (BioTek, USA). To pass all quality criteria, the standard curve R^2 value must be ≥0.98, the spike recovery control 50–200% of the actual glucan concentration, the CV values ≤25% and the last value on the standard curve (0 pg ml^{-1}) must be lower than the next highest standard.

Chromogenic and turbidimetric assay. Associates of Cape Cod, Lonza and Pierce were the manufacturers utilised by the consortium for chromogenic and turbidimetric endotoxin testing. In all cases, the protocol was the same and all controls and quality criteria associated with the ISO and Pharmacopeia standards were met.[15,16] Initially, the endotoxin standard was reconstituted in LAL reagent water and a standard curve was generated based on the sensitivities of the assay (mainly 0.001 EU ml^{-1} or 0.005 EU ml^{-1}). Next, the NM were diluted no further than their calculated maximum valid dilution (MVD), based on the sensitivity of the assay used, the concentration of the NM and the endotoxin limit for a medical device (0.5 EU ml^{-1}).[3,16] At the same dilutions, a known level of endotoxin -within the standard curve- was spiked into each sample for the spike recovery control. 50 μl of standards, samples, spiked controls, quality control (additional endotoxin control) and blank control (LAL reagent water) were added to a 96 well plate in duplicate. Finally, the LAL substrate was reconstituted in either LAL reagent water (for both endotoxin and (1, 3)-β-D-glucan detection) or Glucashield® buffer (for endotoxin-specific detection) and 50 μl was added to each well. The plate was then heated to 37 °C for a predefined period based on the manufacturer's recommendations for the endpoint assay or read immediately in a heated microplate reader for the kinetic assay (types and sources for each group are outlined in ESI Table 1†). For the chromogenic assay, the plate was read at 405 nm; for the turbidimetric assay, the plate was read at 660 nm. To pass all quality criteria, the standard curve R^2

value must be ≥0.98, the spike recovery control 50–200% of the actual endotoxin concentration, the CV values ≤25% and the last value on the standard curve (0 EU ml^{-1}) must be lower than the next highest standard.[15,16]

Gel clot assay. Lonza and Associates of Cape Cod were the manufacturers utilised for gel clot endotoxin testing. Once again, the protocol remained the same in both cases and abided by ISO and Pharmacopeia standards.[15,16] To perform the gel clot assay, 3 tests were undertaken to ensure valid results: initially, a sensitivity validation test was performed to confirm the assay was sensitive to its reported endotoxin concentration (0.03 EU ml^{-1} or 0.06 EU ml^{-1}). This test was undertaken in replicates of four and involved reconstituting the endotoxin and lysate as done for the chromogenic and turbidimetric assays. Standards at 2X, X, 0.5X and 0.25X (where X is the stated sensitivity for the assay) were created and 100 μl of each was added to the gel clot reaction tubes (from the same suppliers), along with 4 tubes containing LAL reagent water as a negative control. Next, the substrate was added at the same volume to each tube and all tubes were heated to 37 °C for 60 min. Following incubation, the tubes were inverted 180° to observe if a clot had been formed. A positive result consisted of a firm clot that was maintained following inversion. Anything other than a firm clot following inversion was considered a negative result. The test was deemed successful if all negative controls failed to clot the gel. From these results, a geometric mean sensitivity for the lysate was calculated by taking the antilog of the mean log endpoint concentrations. If the calculated mean sensitivity was between 50–200% of the stated manufacturer sensitivity, the sensitivity of the lysate was confirmed.

Following this confirmation, a spike-recovery control was performed. Here, the samples were tested at a concentration that does not clot the gel in replicates of four. At this concentration, the samples were spiked with endotoxin at a concentration of 2X, X, 0.5X and 0.25X the sensitivity of the lysate, along with samples alone. In parallel to the spike-recovery control, a sensitivity test was also run again in duplicate as a quality control. For this test to be deemed successful, the samples alone must not clot the gel and the lysate sensitivity must be confirmed again in the parallel test. Additionally, if the lysate retained its sensitivity when endotoxin was added, they were deemed to not interfere with the assay; however, if the sensitivity is outside the 50–200% range then the samples did interfere. If the samples pass the spike-recovery control, they were tested for the quantity of endotoxin they possess in a final test.

For the limit test, the samples were diluted continuously from their stock in LAL reagent water (not exceeding the MVD) and tested in duplicate until no clotting of the gel was observed. At this concentration, an additional test was run with samples alone, samples spiked with 2X the sensitivity of the lysate, an additional 2X control in water and water alone in duplicate. If the spiked sample and water-spiked control were positive, and samples alone and water alone were negative, the limit test was deemed successful and the endotoxin levels were reported.

Recombinant factor C assay. The recombinant factor C assay is a relatively new endotoxin-specific test, with the Food and Drug Administration approving the first drug that utilized this assay for its endotoxin detection in 2018.[21] The principles of the assay are nevertheless the same as the chromogenic and turbidimetric assays,[22] with the reconstitution protocols, controls and quality criteria as described previously (R^2 value ≥0.98, spike recovery control is 50–200% of the actual endotoxin concentration, CV values are ≤25% and the last value on the standard curve (0 EU ml^{-1}) is lower than the next highest standard). The consortium used EndoLISA® and PyroGene™ kits for this assay with sensitivities of 0.005 EU ml^{-1}. Briefly, a standard curve for endotoxin was generated based on the stated sensitivity of the assay (0.005 EU ml^{-1}): 5, 0.5, 0.05, 0.005 and 0 EU ml^{-1}. Then, as before, standards, samples, spike recovery controls, negative and quality controls were added to a 96 well plate in 100 μl volume (note: samples were not diluted beyond the MVD). Next, the assay reagents (fluorogenic substrate, assay buffer and recombinant factor C enzyme) were added with or without washing steps and at different volumes depending on the manufacturer's guidelines. The plate was read fluorescently at 380 nm $_{EX}$/440 nm $_{EM}$ for a time zero reference point. The plate was then incubated based on manufacturers recommendations (37 °C for 60–90 min) and read again at the same wavelengths. The time zero fluorescence was subtracted against the second timepoint to generate the standard curve and calculate the concentrations of each sample and control. The quality criteria for a successful test were the same as the chromogenic and turbidimetric assays.

Statistical analysis

GraphPad version 7 was used to determine statistical distribution (min, mean, max, range and coefficient of variance) of size and contamination results between the consortium.

Results

Physicochemical characterization of nanomaterials

The PCC of the NM used for this interlaboratory study are summarized in Table 1 below and data graphs are provided in ESI Fig. 1–3.† Notably, the IONP had a mean hydrodynamic size range of 79–89 nm, GNP ranged from 128–151 nm and PsNP ranged from 98–116 nm, depending on whether NTA or DLS was used for the analysis. Additionally, each material was monodispersed, with respective polydispersity indexes of 0.111 for IONP, 0.008 for GNP and 0.028 for PsNP, based on DLS measurements. The GNP had a lower stock concentration (0.053 mg ml^{-1}) and so was expected to have a lower particle count (2×10^9 NP ml^{-1}) compared to the IONP (6.46×10^{13} NP ml^{-1}) and PsNP (8.78×10^{13} NP ml^{-1}). All NM were negatively charged at pH 7.5 for IONP and pH 7 for GNP and PsNP. As the IF consisted solely of LAL reagent water that had been exposed to the implant, it was excluded from PCC analysis.

Table 1 Physicochemical characterization of nanomaterials

Sample	NTA mean size (nm)	NTA (NP ml^{-1})	DLS mean size (nm)	DLS PDI	Zeta potential (mV)
IONP	79 ± 0.9	$6.46 \times 10^{13} \pm 1.43 \times 10^{12}$	89	0.111	−13.0 ± 1.2
GNP	128 ± 1.6	$2.08 \times 10^{9} \pm 1.61 \times 10^{8}$	151	0.008	−21.3 ± 2.4
PsNP	98 ± 0.4	$8.78 \times 10^{13} \pm 6.10 \times 10^{11}$	116	0.028	−48.4 ± 1.8

NTA and DLS were used to measure the size distribution of the NM. Dynamic light scattering was also used to measure zeta potential at pH 7.5 for IONP and pH 7 for GNP and PsNP. Abbreviations: NP, nanoparticle; PDI, polydispersity index. Values indicate mean ± standard deviation.

Beta-glucan, microbial and mycoplasma contamination of samples

All samples were assessed for contamination with beta-glucans, microorganisms and mycoplasma. Detectable levels of beta-glucans were noted in the IONP, GNP and PsNP, whereas the levels in the IF were below the lowest value in the standard curve (5 pg ml^{-1}). None of the samples had detectable CFU, indicating sterility (confirming the data provided by the suppliers in each case). Importantly, in both of these cases, the spike-recovery controls for beta-glucan and microbial contamination were within 50–200%, indicating no interference in the tests. Mycoplasma was also considered negative for each sample tested as they produced a reading ratio <0.9, while the positive and negative controls in this test showed positive (34.57) and negative (0.16) ratios, respectively. Importantly, the viability of the cells used for this assay was >98% after incubation with the samples; hence, the samples did not interfere in this regard (Table 2).

Size comparison by the consortium

Hydrodynamic size results from NTA and DLS ensured the NM were not compromised during shipment (Fig. 2). For NTA, IONP had a mean size of 85.9 nm and a standard deviation of 6.7 nm (7.8% CV); GNP had a mean size 127.1 nm and a standard deviation of 1.4 nm (1.1% CV); PsNP had a mean size of 104.3 nm and standard deviation of 5.2 nm (5.0% CV). For

Table 2 Beta-glucan, microbial and mycoplasma contamination of samples

Sample	Beta-glucan contamination (pg ml^{-1})	Spike recovery (%)	Microbial contamination (CFU ml^{-1})	Spike recovery (%)	Mycoplasma reading ratio
IONP	1629.1	103	0	102	0.4011 ± 0.0423
GNP	7.5	96	0	67	0.5134 ± 0.2377
PsNP	4239.3	78	0	108	0.5885 ± 0.1822
IF	<5.0	91	0	71	0.5371 ± 0.0655

Both beta-glucan and microbial contamination levels reflect stock concentrations for each sample. Spike-recovery controls indicate the percentage of the contaminant retrieved following spiking into the sample. Mycoplasma reading ratio refers to the ratio of readings before and after the detection substrate was added to each sample. Abbreviations: CFU, colony forming units.

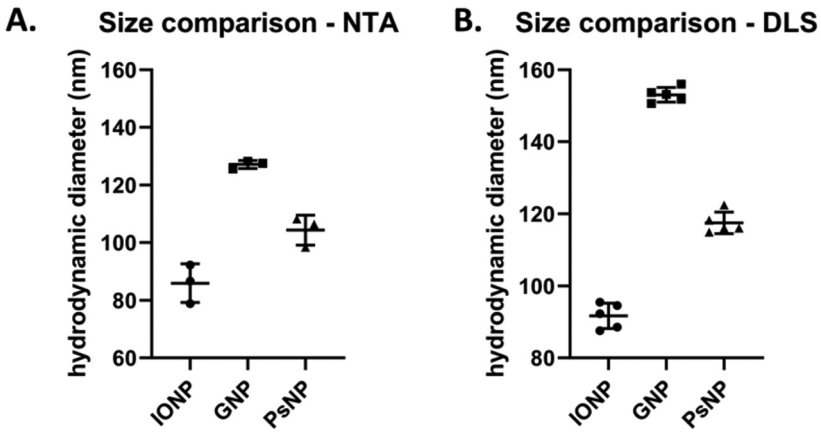

Fig. 2 Size comparison between groups. Bars depict mean hydrodynamic size (nm) ± standard deviation and shapes represent individual results for both NTA and DLS measurements. For NTA, the results are measurements from 3 different groups; for DLS, the results are measurements from 5 different groups.

DLS, IONP had a mean size of 91.7 nm and a standard deviation of 1.6 nm (3.8% CV); GNP had a mean size of 153.1 nm and a standard deviation of 2.0 nm (1.3% CV); PsNP had a mean size of 117.5 nm and a standard deviation of 3.0 nm (2.5% CV).

Endotoxin contamination

The statistical variability of endotoxin results is summarized in Fig. 3 and Table 3. As beta-glucan could be detected for the 3 NM tested, assays for detecting both endotoxin and beta-glucan and endotoxin-specifically were used. All results obtained and reported herein abided by ISO and Pharmacopeia standards for endotoxin assessment of NM (summarized in ESI Table 2†).

The results of endotoxin and beta-glucan quantification reflected seven groups' data for the chromogenic (n = 6) and turbidimetric (n = 2) assays are presented in Fig. 3(A and B) and Table 3. The gel clot assay was also performed by two groups, however, the MVD was reached for the IONP, GNP and PsNP with these assays and values could not be reported. Additionally, the IF levels were below the sensitivity of the assays (0.03 EU ml^{-1}). For the more sensitive LAL assays (chromogenic and turbidimetric), when the endotoxin levels of IF were below the limit of detection they were reported 0.00 EU ml^{-1} in the results. For the NM, specific concentrations could be determined for both the turbidimetric and chromogenic assays in all but one case, where IONP reached the MVD for one turbidimetric assay and could not be reported. IONP had a mean value of 360.1 EU ml^{-1}, but the min and max values of 22.18 EU ml^{-1} and 958.00 EU ml^{-1} respectively noted a large range in the results. This range corresponded to standard deviation of 327.8 EU ml^{-1}. Similar results could also be seen with PsNP, as the mean concentration measured 161.3 EU ml^{-1} and the min and max values were 6.07 EU ml^{-1} and 706.10 EU ml^{-1} respectively. These values equated to a standard deviation of 233.10 EU ml^{-1}. GNP and IF contained considerably less endotoxin (0.90 EU ml^{-1} and 0.02 EU ml^{-1} respectively) and therefore a smaller range in results (0.38–1.17 EU ml^{-1} for

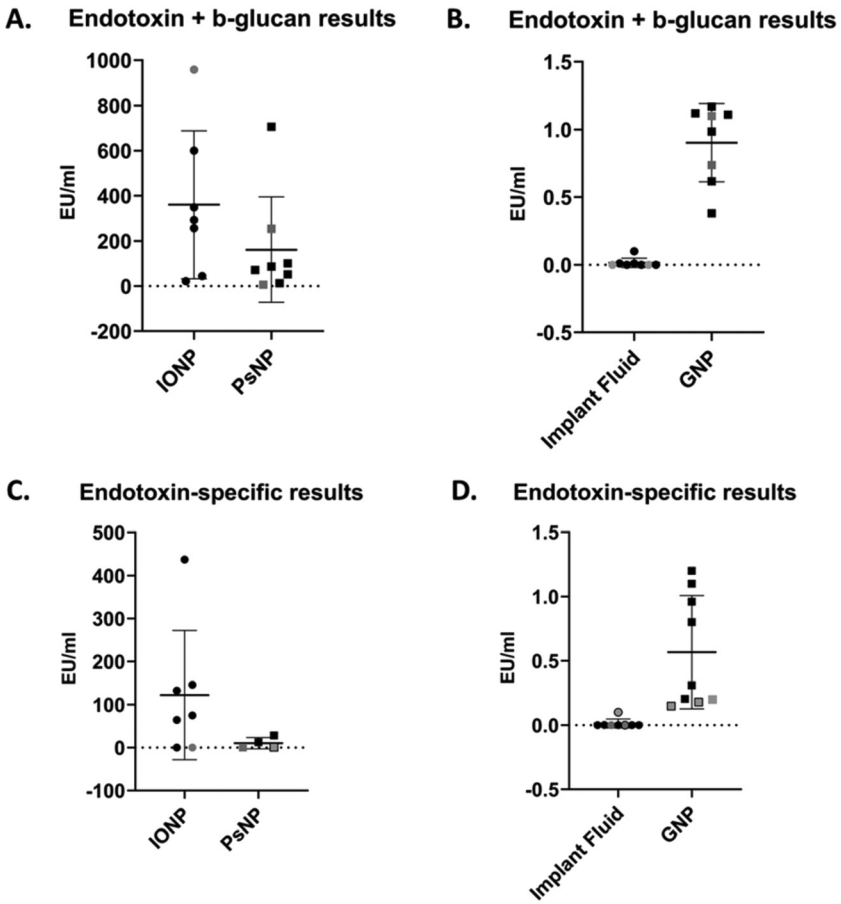

Fig. 3 Summary of results from endotoxin and beta-glucan contamination assessment of samples. (A) Endotoxin and beta-glucan results for IONP (n = 7) and PsNP (n = 8). (B) Endotoxin and beta-glucan results for IF (n = 8) and GNP (n = 8). (C) Endotoxin- specific results for IONP (n = 7) and PsNP (n = 4). (D) Endotoxin- specific results for IF (n = 8) and GNP (n = 9). Lines reflect mean values ± standard deviation and shapes indicate individual results. Black shapes indicate chromogenic assay results, grey shapes indicate turbidimetric assay results and grey shapes with black borders indicate recombinant factor C assay results. Note: for PsNP endotoxin-specific measurements, three values were semi-quantitative and were excluded from this data. These values are specified in ESI Table 2.†

Table 3 Statistical distribution summary for each samples endotoxin and beta-glucan results

Parameter	IONP	PsNP	Implant fluid	GNP
Endotoxin and beta-glucan results (EU ml^{-1})				
Mean	360.10	161.30	0.02	0.90
SD	327.80	233.10	0.04	0.29
Min	22.18	6.07	0.00	0.38
Max	958.00	706.10	0.10	1.17
Range	935.80	700.00	0.10	0.79
CV	91%	145%	231%	32%
Endotoxin-specific results (EU ml^{-1})				
Mean	122.10	10.36	0.00	0.57
SD	150.10	13.17	0.00	0.44
Min	0.005	0.059	0.00	0.15
Max	437.00	28.16	0.1	1.20
Range	432.00	28.16	0.1	1.05
CV	123%	127%	277%	78%

Abbreviations: SD, standard deviation; CV, coefficient of variation.

GNP and 0–0.1 EU ml^{-1} for IF). Accordingly, these materials also exhibited considerably less standard deviation in their data (0.29 EU ml^{-1} for GNP and 0.04 EU ml^{-1} for IF).

The endotoxin-specific results for eight groups' data using the chromogenic (n = 6), turbidimetric (n = 1) and recombinant factor C (n = 2) assays are reported in Fig. 3(C and D) and Table 3. Once again, the gel clot assay was also performed by one group but the MVD was reached for the IONP, GNP and PsNP, and the sensitivity was reached for the IF (0.06 EU ml^{-1}). The IF endotoxin levels were below the level of detection for some groups with the chromogenic, turbidimetric or recombinant factor C assays, and were therefore also reported as 0.00 EU ml^{-1} in the results. Similar findings were observed with PsNP at its MVD for three chromogenic assays, and only ranges for endotoxin could be obtained in these cases. These ranges are provided in ESI Table 2.† Additionally, the recombinant factor C assay was unable to overcome the interference of the IONP in both cases. For both the chromogenic and turbidimetric assays, however, the specific endotoxin concentrations of IONP and GNP could be reported in all cases. IONP had a mean value of 122.10 EU ml^{-1} with a min and max value of 0.005 EU ml^{-1} and 437.00 EU ml^{-1} respectively; PsNP had a mean value of 10.36 EU ml^{-1} with a min and max value of 0.059 EU ml^{-1} and 28.16 EU ml^{-1} respectively. This resulted in standard deviations of 150.10 EU ml^{-1} for IONP and 13.17 EU ml^{-1} for PsNP. As before, GNP and IF contained considerably less endotoxin than the other NM, on average, which resulted in a smaller range of results. GNP had a mean endotoxin centration of 0.57 EU ml^{-1}, with a range of 0.15–1.2 EU ml^{-1} and a standard deviation of 0.44 EU ml^{-1}. The endotoxin levels of IF were undetectable except for two groups, where the concentrations were quantified as 0.002 and 0.1 EU ml^{-1}.

Discussion

Three NM were aliquoted into pyrogen-free tubes and characterized for their PCC by the ILC coordinator prior to batch-shipment to each partner. The fourth material -a medical implant coated with a nanosurface- was exposed to endotoxin-free water and this liquid was also aliquoted for subsequent testing. NTA and DLS were utilised (prior and after shipment) to measure the hydrodynamic size distribution of the NM and the low CV values (<10% in all cases) ensured each sample was not altered during shipment. The zeta potential of each NM -determined by DLS- was negative at pH 7–7.5 and so interference with endotoxin detection assays *via* electrostatic interaction through the negatively-charged phosphate groups on endotoxin could be avoided, as positively charged NM can evoke false negatives in these assays through direct binding to endotoxin.[3]

Next, each sample was tested for microbial and mycoplasma contamination along with presence of beta-glucans. No microbial or mycoplasma contamination was detected for each sample, and confirming this sterility was essential to ensure endotoxin or beta-glucan-harbouring microorganisms were not present in each of the formulations. In IONP, GNP and PsNP, however, beta-glucans could be detected. Notably, IONP and PsNP possessed high levels of beta-glucan within the nanogram range. Beta-glucans are not as potent as endotoxin, but do possess immune-stimulatory properties and are common contaminants in NM.[23,24] Moreover, LAL assays are responsive to both endotoxin and beta-glucans through factor G activity (downstream of endotoxin-specific factor C signalling), and so this contaminant could lead to an overestimation of the endotoxin present in each sample.[23] Because of this, the ILC was expanded to include LAL assays specific to endotoxin along with assays to detect a combination of endotoxin and beta-glucans to compare results between each.

The results for both endotoxin-specific and endotoxin and beta-glucan results varied considerably between groups, particularly for IONP and PsNP. This can be noted with the reported range values, which increased to several hundred EU when the levels of contamination were higher. Importantly, this variation existed even within the same assays, and so this is not a result of inter-assay differences but exists regardless of the assay used. While this large variability range is concerning, it is expected that higher concentrations of endotoxin will lead to greater variations in results as larger dilutions of the NM are required. Therefore, in these cases, if the goal of these assays is to specifically ascertain whether the NM is within endotoxin limits, this large range at higher concentrations is not a major concern.

For the samples with lower endotoxin and beta-glucan contamination -GNP and IF- the range was expectedly lower, however, at this level, small differences were the difference between a pass or fail with regards to regulatory endotoxin limits for medical devices (0.5 EU ml^{-1}). With the endotoxin-specific results, in particular, the GNP and PsNP could pass or fail between assays all while abiding by ISO and Pharmacopeia standards for endotoxin testing of NM. Once again, these differences were not a result of inter-assay variability in the case of GNP, as the same assays were also providing large ranges in results. This is a concerning finding as NM could

potentially harbour greater levels of endotoxin than what has been reported, and this may lead to unexpected immune stimulation at a later point in their preclinical or even clinical evaluation. Notably, mice are 10 000–1 000 000 times less sensitive to pure lipopolysaccharide treatment than humans;[25,26] therefore, the immune-stimulatory effects of a NM containing undetected, excessive levels of endotoxin may go unnoticed until late preclinical or even clinical evaluation.

This variation in results is likely due to the propensity of NM to interfere with LAL assays. While none of these NM were cationic, they all have the potential to influence absorbance at the wavelengths used for the chromogenic, turbidimetric and recombinant factor C assays.[3,12] Moreover, the gel clot assay -that does not use optical absorbance as an endpoint- was an unsuitable alternative for the NM tested here as the MVD was reached in most cases before the endotoxin levels could be quantified. Hence, while current controls are in place in ISO and Pharmacopeia standards to account for the potential of NM to interfere with LAL assays, limitations remain in these tests that may result in misleading findings. The IEC appears not enough to sufficiently determine the extent of NM interference with the LAL assays, and the combination of multiple assay types is advised. This recommendation has also been voiced by the NCI-NCL previously,[13] and its importance is emphasised here as the use of two assays was more likely to pick up a positive result.

The monocyte activation test is the only other regulatory approved, non-animal alternative to the LAL assays.[27] This test also comes with limitations, however, as it also relies on optical absorbance as an endpoint (although NM are mostly washed away prior to detection), the test is not endotoxin-specific and NM with inherent cytotoxicity or immune modulating properties can also interfere with it.[3] It is therefore essential for more work to be carried out in the future to advance the current options for endotoxin assessment of NM.

Conclusion

This study summarized results from an ILC on the endotoxin contamination assessment of four samples containing NM: IONP, GNP, PsNP and a nanosurface- based implant. It was hypothesised that the interference widely reported in the literature with NM and endotoxin assessment would result in variable data between groups, even though ISO and Pharmacopeia quality control standards were met in all cases. While it was ensured that these samples were sterile, and PCC analysis was performed to ensure that none of the samples were altered during batch-preparation and shipment to the various partners, large variations in results were observed, even within the same assays. Notably, for 2 of the 4 samples, individual results showed that each could both pass and fail endotoxin assessment depending on the group performing the assessment. Therefore, this study highlights the limitations of LAL assays to the endotoxin contamination assessment of NM and the need for more work in this space to improve current testing options in the future.

Authors contribution

GH and APM conceptualised and coordinated the study. GH generated data for the study, wrote the initial draft of the manuscript, reviewed subsequent drafts and finalised it for submission. APM reviewed the initial draft, reviewed subsequent drafts, finalised it for submission. BJH, APH, CD, NJL, AE, AAI, NA, OI, AAC, ADPP, NL, IL, FDZ, SZN, AJ, AVD, IN, IA, FA, NV, EGM and AC all contributed equally to the manuscript.

Data availability

The data supporting this article have been included as part of the ESI.†

Conflicts of interest

The authors declare no conflict of interests.

Acknowledgements

This work was funded by the European Commission's Horizon 2020 research and innovation programme (grant agreement: 814607). The authors would also like to acknowledge BioRender software used for the creation of Fig. 1 and the Graphical Abstract.

References

1 A. C. Anselmo and S. Mitragotri, Nanoparticles in the clinic: An update post COVID-19 vaccines, *Bioeng. Transl. Med.*, 2021, **6**(3), e10246.
2 T. J. MacCormack, *et al.*, Commentary: Revisiting nanoparticle-assay interference: There's plenty of room at the bottom for misinterpretation, *Comp. Biochem. Physiol., Part B: Biochem. Mol. Biol.*, 2021, **255**, 110601.
3 G. Hannon and A. Prina-Mello, Endotoxin contamination of engineered nanomaterials: Overcoming the hurdles associated with endotoxin testing, *WIREs Nanomed. Nanobiotechnol.*, 2021, **13**(6), e1738.
4 S. E. Calvano and S. M. Coyle, Experimental Human Endotoxemia: A Model of the Systemic Inflammatory Response Syndrome?, *Surg. Infect.*, 2012, **13**(5), 293–299.
5 J. N. Fullerton, *et al.*, Intravenous Endotoxin Challenge in Healthy Humans: An Experimental Platform to Investigate and Modulate Systemic Inflammation, *J. Visualized Exp.*, 2016, (111), e53913.

6 S. Taudorf, *et al.*, Human Models of Low-Grade Inflammation: Bolus versus Continuous Infusion of Endotoxin, *Clin. Vaccine Immunol.*, 2007, **14**(3), 250–255.
7 R. M. Crist, *et al.*, Common pitfalls in nanotechnology: lessons learned from NCI's Nanotechnology Characterization Laboratory, *Integr. Biol.*, 2013, **5**(1), 66–73.
8 G. Hannon, *et al.*, Immunotoxicity Considerations for Next Generation Cancer Nanomedicines, *Adv. Sci.*, 2019, **6**(19), 1900133.
9 Y. Li and D. Boraschi, Endotoxin contamination: a key element in the interpretation of nanosafety studies, *Nanomedicine*, 2016, **11**(3), 269–287.
10 Y. Li, M. Fujita and D. Boraschi, Endotoxin Contamination in Nanomaterials Leads to the Misinterpretation of Immunosafety Results, *Front. Immunol.*, 2017, **8**, 472.
11 Y. Li, *et al.*, Bacterial endotoxin (lipopolysaccharide) binds to the surface of gold nanoparticles, interferes with biocorona formation and induces human monocyte inflammatory activation, *Nanotoxicology*, 2017, **11**(9–10), 1157–1175.
12 Y. Li, *et al.*, Optimising the use of commercial LAL assays for the analysis of endotoxin contamination in metal colloids and metal oxide nanoparticles, *Nanotoxicology*, 2015, **9**(4), 462–473.
13 M. A. Dobrovolskaia, Pre-clinical immunotoxicity studies of nanotechnology-formulated drugs: Challenges, considerations and strategy, *J. Controlled Release*, 2015, **220**(Pt B), 571–583.
14 M. Mangini, *et al.*, Interaction of nanoparticles with endotoxin Importance in nanosafety testing and exploitation for endotoxin binding, *Nanotoxicology*, 2021, **15**(4), 558–576.
15 ISO, Nanotechnologies:Endotoxin test on nanomaterial samples for in vitro systems: Limulus amebocyte lysate (LAL) test. 2010.
16 USP, <85> Bacterial Endotoxin Test. 2012.
17 M. A. Dobrovolskaia, D. R. Germolec and J. L. Weaver, Evaluation of nanoparticle immunotoxicity, *Nat. Nanotechnol.*, 2009, **4**(7), 411–414.
18 EUNCL. Measuring Batch Mode DLS., 2016[cited 2023 January]; Available from: **https://www.euncl.org/about-us/assay-cascade/PDFs/Prescreening/EUNCL-PCC-001.pdf?m=1468937875&**.
19 EUNCL. Particle Tracking Analysis. 2018[cited 2023 January]; Available from: **https://www.euncl.org/about-us/assay-cascade/PDFs/PCC/EUNCL_PCC_023.pdf?m=1526712237&**.
20 EUNCL. Detection of Bacterial Contamination by Agar Plate Test. 2016[cited 2023 January]; Available from: **https://www.euncl.org/about-us/assay-cascade/PDFs/Prescreening/EUNCL-STE-002_2.pdf?m=1476164583&**.
21 USP. USP provides guidelines for Recombinant Factor C (rFC) a non-animal-derived reagent critical to development of vaccines and other sterile pharmaceutical products. 2020[cited 2023 January]; Available from: **https://www.usp.org/news/rfc-horseshoe-crabs-statement**.
22 H. Grallert, *et al.*, EndoLISA®: a novel and reliable method for endotoxin detection, *Nat. Methods*, 2011, **8**(10), iii–v.
23 B. W. Neun, *et al.*, Detection of Beta-Glucan Contamination in Nanotechnology-Based Formulations, *Molecules*, 2020, **25**(15), 3367.
24 B. Han, *et al.*, Structure-Functional Activity Relationship of β-Glucans From the Perspective of Immunomodulation: A Mini-Review, *Front. Immunol.*, 2020, **11**, 658.
25 J. Lasselin, *et al.*, Comparison of bacterial lipopolysaccharide-induced sickness behavior in rodents and humans: Relevance for symptoms of anxiety and depression, *Neurosci. Biobehav. Rev.*, 2020, **115**, 15–24.
26 H. S. Warren, *et al.*, Resilience to bacterial infection: difference between species could be due to proteins in serum, *J. Infect. Dis.*, 2010, **201**(2), 223–232.
27 T. Hartung, Pyrogen testing revisited on occasion of the 25th anniversary of the whole blood monocyte activation test, *ALTEX - Alternatives to animal experimentation*, 2021, **38**(1), 3–19.